Generated Pattern Current for Hybrid Capacitor Production Activation: Pore Access, Contact Stabilization, and Electrode Balancing

Ibrahim Karakoc

GigaPulse Energy, Izmir, Turkey | ibrahim@gigapulse.energy

PCT/TR2025/051176 | USPTO Appl. No. 19/298,223 | Priority Date: July 23, 2025

Abstract

Hybrid capacitors (HyCap) combine a battery-type faradaic electrode with a capacitor-type non-faradaic electrode (electrical double-layer capacitor, EDLC) to achieve simultaneous high energy and high power density. After manufacturing, these devices require an activation process typically lasting 10 to 50 cycles before reaching full performance. During activation, three concurrent physical phenomena must be addressed: electrolyte infiltration and pore access within hierarchical carbon structures, graphene flake contact network stabilization through micro-annealing, and balancing of the two electrodes that operate at fundamentally different time constants. Conventional constant-current or constant-voltage activation applies a uniform temporal stimulus that cannot independently address these three phenomena.

This paper presents the application of the Generated Pattern Current (GPC) paradigm, implemented through the Dynamic Defined Pattern Charging (DDPC) framework, to HyCap production activation. GPC controls activation through three mechanisms: diffusion relaxation during low-current intervals enables homogeneous ion distribution into deep pores; controlled micro-annealing through I^2Rc pulse modulation stabilizes graphene contact percolation networks; and frequency decoupling delivers stimulation at the characteristic timescale of each electrode type. Theoretical analysis and electrochemical modeling indicate potential reductions of 60–70% in activation cycle count, 10–20% reduction in equivalent series resistance, and 5–10% improvement in usable capacitance. The GigaPulse Lab platform provides a reference implementation supporting pattern library execution and closed-loop activation feedback.

Keywords: Generated Pattern Current (GPC); Dynamic Defined Pattern Charging (DDPC); hybrid capacitor; supercapacitor activation; graphene electrode; pore access; contact resistance; EDLC; faradaic electrode; equivalent series resistance; percolation network

1. Introduction

1.1 Background and Motivation

Hybrid capacitors represent a convergence of two electrochemical storage paradigms: the high energy density of battery-type intercalation electrodes and the high power density of electrical double-layer capacitors [1,2]. This convergence is achieved by pairing a faradaic electrode—typically lithium intercalation carbon or metal oxide—with a non-faradaic activated carbon or graphene electrode in a common electrolyte [3]. The resulting devices occupy the Ragone space

between conventional batteries and EDLCs, making them particularly attractive for applications requiring rapid charge delivery combined with moderate energy storage: regenerative braking, grid frequency response, pulse-power industrial drives, and portable electronics [4].

Despite the favorable theoretical characteristics of hybrid capacitors, the transition from manufactured device to fully performing device is not immediate. A process known as activation—repeated charge and discharge cycling under controlled conditions—is required to bring the device to its rated performance. This activation step is routinely performed in HyCap production lines and typically requires 10 to 50 full cycles before the device stabilizes. The cost of activation time, energy consumed during activation, and variability in the final ESR distribution across a production batch are recognized inefficiencies in HyCap manufacturing [5]. Reducing the required number of activation cycles while simultaneously improving the uniformity of the activated state is therefore of direct industrial and scientific relevance.

1.2 Limitations of Conventional Activation

The standard activation protocol applies constant-current (galvanostatic) or constant-voltage (potentiostatic) cycling within defined voltage windows. This approach treats the device as a lumped circuit element and applies a temporally uniform stimulus. However, the physical processes occurring inside a HyCap during activation are neither uniform nor simultaneous [6]. Ion transport into micropores operates on diffusion timescales governed by pore geometry; graphene contact network stabilization is a thermally driven process sensitive to instantaneous I^2R heating; and the two electrodes that constitute the device have fundamentally different response times. A constant-current waveform cannot independently address these three processes. It necessarily optimizes for none of them.

The scientific literature on HyCap activation predominantly addresses the problem from a materials perspective: electrode porosity engineering, electrolyte formulation, and binder composition are adjusted to reduce the number of activation cycles required [7,8]. The temporal structure of the activation current—the parameter most directly controllable in a production environment—has not been treated as a primary design variable. This paper addresses that gap.

1.3 The Generated Pattern Current Framework

Generated Pattern Current (GPC) is an electrical control paradigm in which the temporal structure of the delivered current is designed to match the physical response characteristics of the target electrochemical system [9]. GPC is defined and protected under PCT/TR2025/051176 and USPTO Application No. 19/298,223 (priority date July 23, 2025). The core formalism derives from Jensen's inequality applied to nonlinear electrochemical systems: for a nonlinear response function f, the response to a temporally structured current $f(I(t))$ is not equal to the response to the time-averaged current $f(\bar{I})$, where $\bar{I}$ is the mean value. Temporal structure carries physical information that time-averaging destroys.

GPC has been applied across multiple electrochemical domains: lithium-ion battery formation, charging optimization, photovoltaic panel activation, and fuel cell conditioning. Each application demonstrates that designing the temporal current profile to match the characteristic

timescales of the target system produces measurable improvements in outcomes compared to temporally uniform approaches. Hybrid capacitor activation presents a particularly well-suited application domain because of the three concurrent, timescale-separated physical processes involved.

1.4 Scope of This Paper

This paper presents the theoretical framework for GPC-based HyCap activation. Section 2 describes the relevant electrode physics, including dual storage mechanisms, ESR components, and pore structure. Section 3 analyzes the three activation dynamics that GPC targets. Section 4 presents the GPC activation protocol design. Section 5 quantifies expected outcomes. Section 6 describes the experimental validation framework and the GigaPulse Lab reference implementation. Section 7 concludes.

2. Hybrid Capacitor Electrode Physics

2.1 Dual Storage Mechanism and Time Constant Separation

The non-faradaic EDLC electrode stores charge through electrostatic adsorption at the electrode–electrolyte interface. The capacitance is given by $C = \varepsilon A/d$, where ε is the electrolyte permittivity, A is the accessible electrochemical surface area, and d is the effective double-layer thickness. This process is inherently fast, operating on microsecond to millisecond timescales, limited primarily by ion transport to the electrode surface [10]. Activated carbon or graphene with high specific surface area (500–2000 m^2/g) provides the electrode material [11,12].

The faradaic electrode stores charge through reversible ion intercalation or surface redox reactions. These processes involve ionic diffusion into bulk electrode material and phase transitions, operating on timescales of seconds to minutes depending on electrode thickness and ion diffusivity [13]. The time constant separation between the two electrodes is therefore:

$$\tau_{EDLC} \ll \tau_{faradaic}$$

Under constant-current activation, both electrodes receive the same temporal stimulus simultaneously. The EDLC electrode responds to the full bandwidth of the applied signal, while the faradaic electrode integrates over it. The consequence is that the optimal stimulus for each electrode cannot be simultaneously applied through a single constant-current profile. GPC's frequency decoupling addresses this fundamental constraint [14].

2.2 Equivalent Series Resistance Components

The total equivalent series resistance of a hybrid capacitor determines its power delivery capability. ESR is the sum of three main contributions [15]:

$$R_{ESR} = R_{ion} + R_{contact} + R_{collector}$$

where R_{ion} is the ionic transport resistance through the electrolyte and within electrode pores, $R_{contact}$ is the graphene flake contact resistance arising from the percolation network of the

carbon electrode, and R_collector is the interface resistance between the active electrode material and the current collector. Each component is influenced differently by the activation process. R_ion is primarily governed by pore accessibility and electrolyte wetting. R_contact is a function of the graphene percolation network state and can be modified by controlled thermal treatment of contact junctions. R_collector is determined by the electrode fabrication quality and is largely fixed at assembly [16].

The total ESR determines the heat generated per unit time during discharge ($P_{loss} = I^2 \cdot R_{ESR}$) and the power available for delivery ($P_{available} = V_{oc}^2 / (4 \cdot R_{ESR})$ at matched load). Minimizing R_ESR, and particularly achieving a narrow ESR distribution across a production batch, is therefore a central objective of the activation process. Cell-to-cell ESR variance propagates into module-level performance degradation when cells are connected in series or parallel strings.

2.3 Hierarchical Pore Structure and Ion Access Dynamics

High-performance EDLC and HyCap electrodes utilize hierarchical pore structures combining macropores (>50 nm), mesopores (2–50 nm), and micropores (<2 nm) [17]. Macropores serve as ion-transport highways; mesopores provide both transport and capacitance; micropores deliver the highest capacitance per unit volume but present the greatest ion transport resistance [18]. The wetting time for pores of depth L is governed by:

$$t_{wet} \sim L^2 / D_{eff}$$

where D_eff is the effective ion diffusivity in the pore, which is itself a function of pore diameter and electrolyte concentration. For deep micropores, wetting times can exceed surface pore wetting times by two to three orders of magnitude. Under constant-current activation, the surface electrode area saturates within the first few cycles, while deep micropores continue to activate over many subsequent cycles. This sequential activation is a primary driver of the observed 10–50 cycle requirement. A current profile that alternates between high-current injection phases (driving ions into the pore structure) and low-current relaxation phases (allowing diffusive redistribution) can substantially accelerate this process [19].

2.4 Graphene Percolation Network Physics

Graphene-based EDLC electrodes are fabricated by coating current collectors with graphene flake dispersions combined with polymer binders. The resulting structure is a percolation network of overlapping graphene flakes with finite contact resistance at each junction [20]. The network resistance evolves during activation through a mechanism analogous to electrical sintering: repeated I^2R_c heating at contact points drives local thermal annealing, improving flake alignment, reducing interflake resistance, and creating more conductive percolation paths [21,22]. This contact resistance evolution follows the dynamic equation:

$$dR_c/dt = -k_1 \cdot I(t)^2 \cdot R_c + k_2 \cdot T$$

where k_1 is the annealing rate coefficient, R_c is the instantaneous contact resistance, k_2 is a thermal expansion coefficient, and T is the local temperature. Under constant current, this process proceeds uniformly but without the controlled thermal relaxation that allows

mechanical stabilization of the improved contact geometry. GPC's pulse structure creates discrete micro-annealing events followed by controlled relaxation intervals, enabling more systematic contact network evolution [23].

3. Three Concurrent Activation Dynamics Targeted by Generated Pattern Current

3.1 Diffusion Relaxation for Pore Access Homogenization

Ion transport within a hierarchical porous electrode during activation is governed by the modified diffusion equation:

$$\partial c/\partial t = D\nabla^2 c + f(I(t))$$

where c is local ion concentration, D is the diffusion coefficient tensor accounting for pore geometry, and f(I(t)) is the source term proportional to the applied current. Under constant current, f(I(t)) is constant, driving a steady concentration gradient that favors surface pore population over deep micropore penetration. Surface pores saturate; deep pores remain partially starved. The result is that available surface area is underutilized in early activation cycles, and additional cycles are required to progressively access deep electrode volume.

Under a GPC diffusion relaxation pattern, the current profile consists of a high-current injection phase followed by a low-current relaxation interval. During the high-current phase, ions are injected into the accessible pore volume. During the low-current phase, the applied current source term is reduced, allowing the existing concentration gradient to drive diffusion of ions from surface pores into deep micropores. This is the principle of diffusion relaxation: the deliberate creation of a low-current interval allows the system to use its stored concentration gradient productively. Repeated over many cycles, this mechanism systematically extends the depth of electrode activation and reduces the total number of cycles required to achieve full pore utilization [3,19].

Figure 1. Pore Ion Access: Constant Current vs GPC Pattern Activation — Schematic

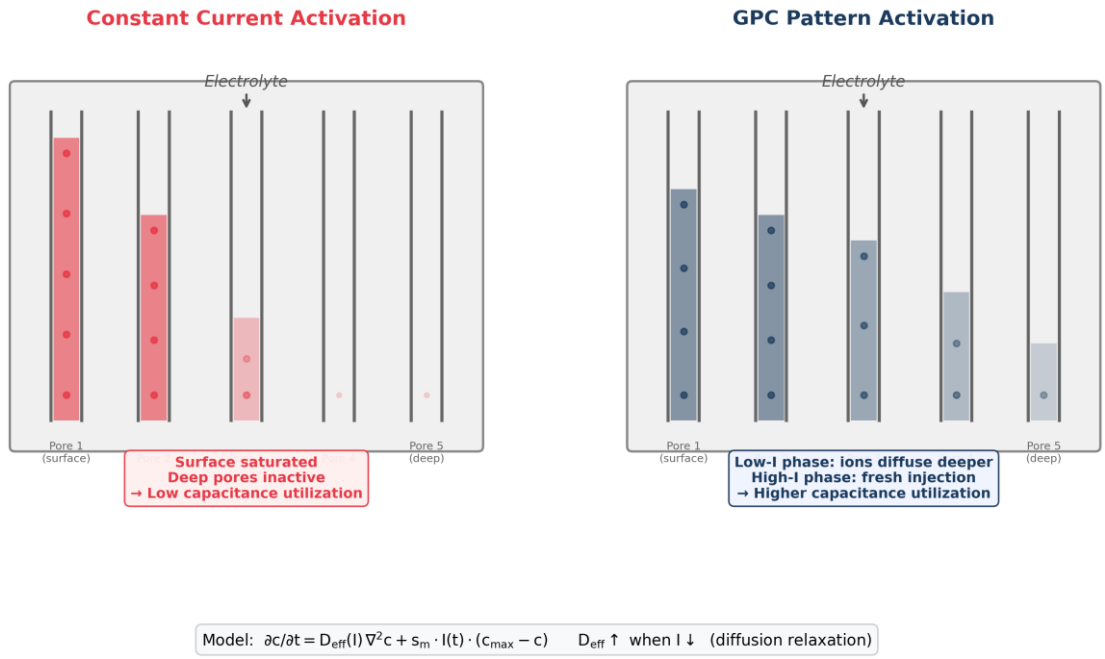

Figure 1. Pore ion access dynamics under constant current versus GPC diffusion relaxation pattern. Schematic of concentration profiles at three time points.

3.2 Controlled Micro-Annealing for Contact Network Stabilization

The percolation network resistance reduction described in Section 2.4 proceeds through local I²R_c heating at graphene flake contact junctions. This thermal process is beneficial—it reduces R_contact and improves the conductivity of the electrode—but it is not irreversible under all conditions. If thermal expansion during a heating pulse is not followed by a controlled relaxation period, mechanical stress at contact junctions can partially undo the achieved improvement or introduce fatigue damage in the graphene structure [24].

GPC-based micro-annealing addresses this through deliberate pulse shaping: high-current pulses are followed by rest intervals whose duration and amplitude are chosen to allow thermal relaxation to ambient temperature before the next heating pulse. The result is a stepwise improvement of the contact network: each pulse achieves an increment of annealing, and each relaxation interval preserves that increment. The cumulative effect is a more homogeneous percolation network with lower R_contact variance across the electrode area. This directly reduces cell-to-cell ESR variance in production batches [25].

Figure 2. Graphene Flake Contact Network: Constant vs GPC Activation — Schematic

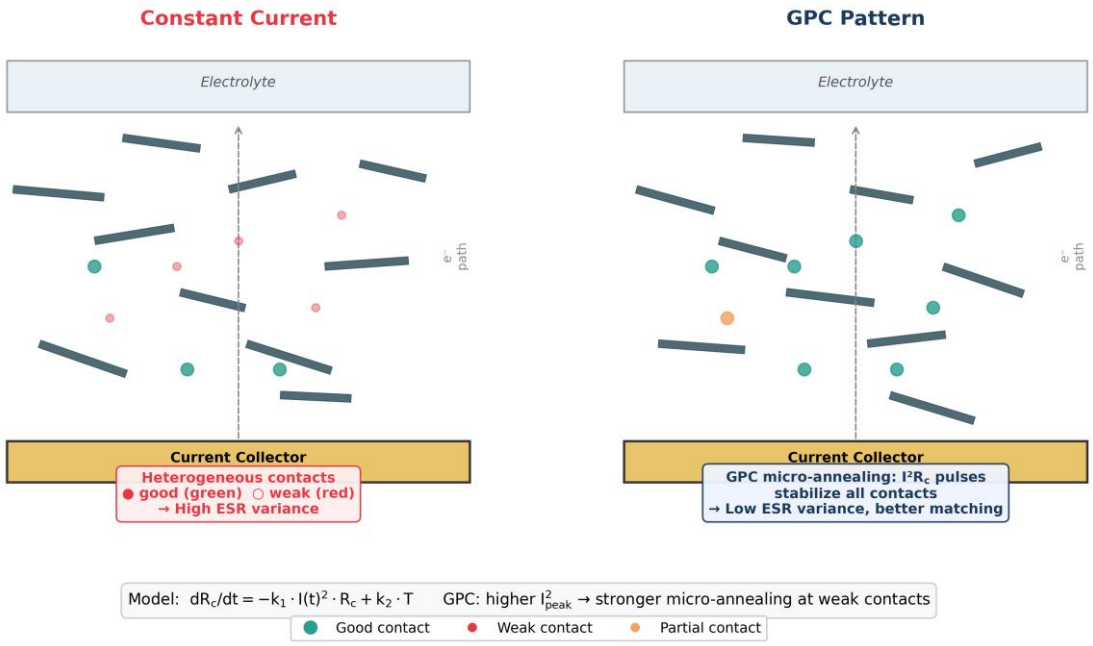

Figure 2. Graphene contact network evolution under constant current versus GPC micro-annealing pattern. Schematic cross-sections at initial, intermediate, and final states.

3.3 Frequency Decoupling for Dual-Electrode Addressing

The time constant separation between the EDLC and faradaic electrodes ($\tau_{EDLC} \ll \tau_{faradaic}$) provides a natural basis for frequency-domain electrode addressing. A GPC composite pattern can simultaneously carry multiple frequency components within a single current profile:

$$I(t) = I_{dc} + I_{HF} \cdot \sin(2\pi f_{HF} \cdot t) + I_{LF} \cdot \sin(2\pi f_{LF} \cdot t)$$

where I_{dc} is the baseline charging current, I_{HF} is the amplitude of the high-frequency component targeting the EDLC electrode, and I_{LF} is the amplitude of the low-frequency component targeting the faradaic electrode. The frequency selection follows:

$f_{HF} \sim 1/\tau_{EDLC}$ *(EDLC pore conditioning)*

$f_{LF} \sim 1/\tau_{faradaic}$ *(faradaic electrode intercalation)*

This design allows a single current waveform to simultaneously drive EDLC pore conditioning at the EDLC's natural response frequency and faradaic intercalation at the intercalation process's natural timescale. The two electrodes receive stimulation optimized for their respective physics within a single unified protocol. This approach is distinct from single-frequency AC superposition techniques reported in the literature for battery applications; it is specific to the dual-electrode architecture of hybrid capacitors [13,14].

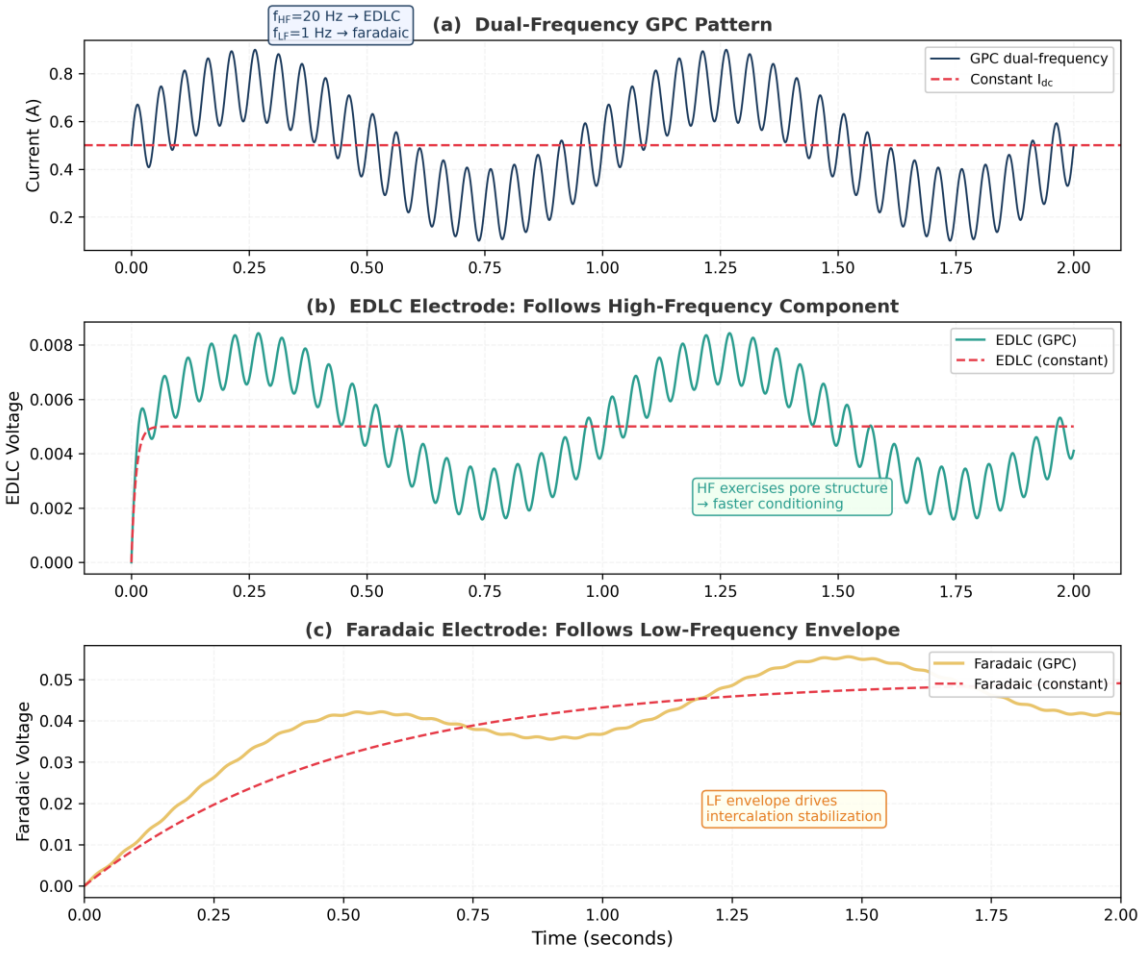

Figure 3. Frequency Decoupling for Two-Electrode HyCap — Model-derived

Figure 3. Frequency decoupling GPC pattern. (a) Composite current profile I(t) = I_dc + I_HF + I_LF. (b) EDLC electrode response dominated by high-frequency component. (c) Faradaic electrode response tracking low-frequency envelope. Model-derived illustration.

4. Generated Pattern Current Activation Protocol Design

4.1 Pattern Architecture

A complete GPC-based HyCap activation protocol integrates all three mechanisms described in Section 3 into a unified current profile. The protocol is defined by the following parameter set: base current I_dc (determined by the C-rate equivalent for activation), high-frequency component amplitude I_HF and frequency f_HF, low-frequency component amplitude I_LF and frequency f_LF, relaxation interval duty cycle D_relax, and total protocol duration expressed in equivalent cycles.

The parameter selection process begins with characterization of the target HyCap type: electrode materials, pore size distribution (from BET analysis), electrolyte ionic conductivity, and the approximate time constants of the two electrode types. These inputs determine the frequency targets for the decoupling components and the diffusion relaxation interval duration. The GigaPulse Lab platform provides a calibration workflow for parameter selection based on

device characterization data, generating application-specific calibration files for each HyCap product type.

4.2 Diffusion Relaxation Implementation

The diffusion relaxation mechanism is implemented as a periodic current reduction to a value $I_{relax} = \alpha \cdot I_{dc}$, where α is a dimensionless relaxation factor (typically 0.05 to 0.15), applied for a relaxation interval t_{relax}. The relaxation interval duration is set to:

$$t_{relax} \sim L_{max}^2 / (2 \cdot D_{eff})$$

where L_{max} is the characteristic depth of the deepest pore category in the electrode. This ensures that during each relaxation interval, a significant fraction of the concentration gradient accumulated during the preceding injection phase is redistributed toward deep pores. The ratio of injection phase duration to relaxation interval duration determines the overall charging rate—a longer relaxation interval provides better ion distribution at the cost of slower charging. In production applications, this ratio is a tunable parameter that can be optimized for the production cycle time constraint.

4.3 Micro-Annealing Pulse Specification

The micro-annealing component consists of short-duration high-current pulses superimposed on the base current profile. The pulse amplitude I_{pulse} is set to produce a target contact junction temperature increment $\Delta T_{junction}$ according to the thermal model:

$$\Delta T = I_{pulse}^2 \cdot R_c \cdot R_{thermal} \cdot t_{pulse}$$

where $R_{thermal}$ is the thermal resistance of the contact junction and t_{pulse} is the pulse duration. The target temperature increment is chosen to be above the minimum effective annealing threshold for graphene contacts (typically 50–80°C above ambient at the junction) but below the electrolyte decomposition temperature. The inter-pulse rest interval ensures junction cooling before the next pulse.

In practice, the thermal parameters of graphene contact junctions are not directly measurable in a production setting. The GigaPulse Lab implementation uses the real-time stress index measurement—derived from the instantaneous ESR monitored via impedance spectroscopy—as a proxy for the state of the contact network, and adjusts pulse amplitude accordingly through closed-loop feedback.

4.4 Integration of Three Mechanisms

The three mechanisms—diffusion relaxation, micro-annealing, and frequency decoupling—operate on different timescales and can therefore be layered into a single current profile without interference. Frequency decoupling operates in the frequency domain (distinct f_{HF} and f_{LF} components); diffusion relaxation operates on the medium timescale of a few seconds; micro-annealing pulses operate on the short timescale of milliseconds to tens of milliseconds. The GPC pattern generator constructs the composite profile by superimposing these components according to the parameter set determined in the calibration workflow.

This layered architecture is the key advantage of the GPC paradigm for HyCap activation: a single current profile, executable on standard activation equipment equipped with a programmable current source, simultaneously addresses all three rate-limiting processes of HyCap activation. No additional hardware beyond the current source modification and the GigaPulse Lab control interface is required.

5. Activation Metrics and Expected Outcomes

5.1 Cycle Reduction

The primary production metric for HyCap activation efficiency is the number of activation cycles required to bring the device to within a defined percentage (typically 98–99%) of its rated capacitance and within specified ESR limits. The GPC efficiency factor for HyCap is defined as:

$$\Psi_{GP,HC} = n_{cycles,ref} / n_{cycles,GP}$$

where n_cycles,ref is the number of cycles required under constant-current activation and n_cycles,GP is the corresponding number under GPC activation. Based on the three mechanisms described in Sections 3 and 4, the expected efficiency factor falls in the range Ψ_GP,HC = 2 to 5, corresponding to a 50–80% reduction in activation cycle count. The dominant contribution comes from diffusion relaxation accelerating deep pore access; micro-annealing and frequency decoupling provide additional but smaller contributions.

5.2 ESR Reduction and Variance Narrowing

ESR improvement under GPC activation has two components. First, lower R_ion through more complete pore wetting. Second, lower R_contact through more controlled graphene contact network annealing. The combined effect is expected to produce a 10–20% reduction in mean ESR compared to constant-current activation baseline, and a reduction in cell-to-cell ESR standard deviation of 30–50%. The latter is particularly important for module assembly: tighter ESR distribution reduces the voltage imbalance and thermal gradient across series-connected cell strings.

5.3 Capacitance Improvement

The accessible capacitance of a HyCap is proportional to the electrochemically active surface area that has been wetted and activated. Incomplete pore access under constant-current activation leaves a portion of the electrode's theoretical capacitance unused. GPC-driven homogeneous pore activation is expected to increase usable capacitance by 5–10% relative to the constant-current baseline, corresponding to more complete utilization of the available electrode surface area [7,8].

Parameter	Constant Current	GPC Activation
Activation cycles to rated capacitance	10–50	3–10 (60–80% reduction)
Capacitance utilization (relative)	Reference	+5–10%

Mean ESR (relative)	Reference	−10–20%
Cell-to-cell ESR standard deviation	Wide distribution	30–50% narrower
Power density (relative)	Reference	Improved (R_ESR reduced)
Ψ_GP,HC efficiency factor	1.0 (by definition)	2–5× cycle reduction

Table 1. Expected outcomes of GPC-based HyCap activation compared to constant-current baseline.

6. Experimental Validation Framework and Reference Implementation

6.1 GigaPulse Lab as Reference Implementation Platform

The GigaPulse Lab platform serves as the reference implementation for GPC-based HyCap activation. The platform provides a complete pattern execution environment designed for electrochemical applications: a full GPC pattern library including Sinusoidal, SuperPulse, Gaussian, ChemPat, and custom lookup-table (LUT) profiles; closed-loop feedback control enabling real-time adjustment of pattern parameters based on measured cell response; a real-time stress index derived from continuous impedance spectroscopy; and application-specific calibration files for different HyCap product types.

For HyCap activation, the GigaPulse Lab platform configures the activation station to execute the composite GPC pattern described in Section 4, monitors ESR evolution in real time, and terminates the activation protocol when the convergence criterion (ESR below threshold, capacitance above threshold, inter-cycle variance below threshold) is satisfied. This adaptive termination replaces the fixed cycle count of conventional activation, further reducing the average activation energy and time in production.

The platform's LUT-based pattern generation allows arbitrary current profiles to be defined and reproduced with high temporal fidelity. The calibration workflow generates HyCap-type-specific parameter files that can be distributed across multiple production stations, ensuring activation consistency across a manufacturing line. The reference implementation is described in detail in the companion patent filings PCT/TR2025/051176 and USPTO 19/298,223.

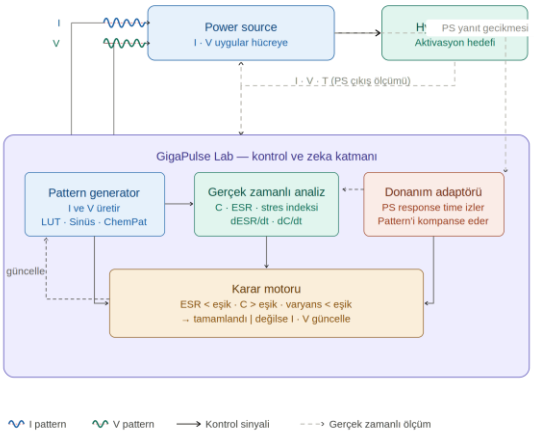

Figure 4. GPC tabanlı HyCap aktivasyonu sistem mimarisi. GP Lab = kontrol katmanı, güç kaynağı değil.

Figure 4. GPC-based HyCap activation system architecture. GP Lab is the control and intelligence layer, not a power supply. I and V pattern signals are applied to the Power Source input terminals; real-time measurements feed back to GP Lab for closed-loop control and process completion decisions.

6.2 Proposed Experimental Protocol

Independent experimental validation of GPC-based HyCap activation requires a controlled comparison between constant-current and GPC activation protocols applied to identical HyCap devices. The proposed protocol is as follows. A batch of commercially available hybrid capacitors—such as lithium-ion capacitors (LIC) or graphene-based asymmetric supercapacitors—is divided into two equal groups with matched initial impedance. The control group undergoes standard constant-current activation at the manufacturer-specified rate. The experimental group undergoes GPC activation using parameters determined from the calibration workflow.

Measurements after each activation cycle include: capacitance from galvanostatic charge–discharge at constant current (C), equivalent series resistance from electrochemical impedance spectroscopy (EIS) at 1 kHz, power density from Ragone characterization, and cycle efficiency defined as energy_out / energy_in. At defined cycle milestones (cycles 1, 3, 5, 10, 20, 30, 50 or until convergence), full Ragone plots are constructed. The primary endpoint is the cycle number at which the device reaches 98% of its rated capacitance while satisfying the ESR specification.

6.3 Accessible Experimental Formats

HyCap activation experiments are accessible to any laboratory equipped with a battery cycler capable of programmable current profiles. The GPC patterns described in this paper can be approximated on commercial cyclers (e.g., Neware, Maccor, BioLogic) by uploading the composite current profile as a step sequence. For higher temporal fidelity, particularly for the high-frequency components of the frequency decoupling pattern, a programmable current source with bandwidth exceeding the highest pattern frequency is required. The GigaPulse Lab platform provides this capability as its reference implementation; researchers who wish to validate independently can implement equivalent functionality using laboratory-grade arbitrary waveform generators connected to a power stage appropriate for the cell current range.

The authors encourage independent experimental validation by researchers with access to HyCap production environments, battery test laboratories, or university electrochemistry facilities equipped with EIS measurement capability. The theoretical predictions in Table 1 are designed as quantitative targets for validation experiments and will be refined as experimental data become available.

7. Discussion

7.1 Comparison with Related Activation Approaches

Several techniques for accelerating capacitor formation and activation have been reported in the literature. Temperature-assisted activation exploits the exponential dependence of ion

diffusivity on temperature to accelerate pore wetting and contact annealing simultaneously [5,6]. While effective, elevated-temperature activation introduces risks of electrolyte decomposition and SEI instability, and requires thermal management infrastructure not present on standard activation lines.

Alternating current preconditioning, in which a sinusoidal AC signal is superimposed on the DC activation current, has been shown to improve pore access in EDLC electrodes by driving oscillatory ion motion [18]. This approach addresses the diffusion relaxation mechanism but does not provide frequency decoupling between the two electrodes or the pulse-shaped micro-annealing of contact networks. GPC generalizes the AC superposition concept by allowing arbitrary temporal structures, enabling simultaneous optimization of all three activation dynamics.

Voltage-step activation protocols, in which the activation voltage window is progressively expanded over cycles, address SEI formation in lithium-intercalation faradaic electrodes but do not influence the EDLC pore access or contact network stabilization mechanisms. GPC is complementary to voltage-window protocols and can be applied within any voltage sequence.

7.2 Generalization Across HyCap Chemistries

The three activation dynamics described in this paper—pore access, contact stabilization, and electrode balancing—are not specific to a single HyCap chemistry. Lithium-ion capacitors (faradaic electrode: pre-lithiated hard carbon; EDLC electrode: activated carbon) exhibit both pore access requirements and the dual time constant separation. Graphene-based asymmetric supercapacitors exhibit all three dynamics due to the graphene percolation network structure. Pseudocapacitive hybrid devices, in which one electrode stores charge through surface redox reactions rather than bulk intercalation, may exhibit different effective time constants but the same frequency decoupling principle applies: f_LF is set to match the characteristic timescale of the redox process rather than bulk intercalation [12,13].

The GPC parameter set—f_HF, f_LF, I_HF, I_LF, t_relax, D_relax—can be calibrated for each specific HyCap chemistry using the procedure described in Section 4.1. The framework is therefore a general activation methodology rather than a chemistry-specific protocol.

7.3 Industrial Deployment Considerations

Industrial deployment of GPC-based activation requires modification of the activation station current source to support programmable profile execution. Existing activation equipment from major manufacturers (Arbin, Neware, PEC) can be retrofit with external current source modulation through their auxiliary input interfaces. For new equipment procurement, the GigaPulse Lab integration provides a direct implementation path. The energy cost of GPC activation is not significantly different from constant-current activation at the same average current, since the time-averaged current is identical by design. The production benefit is entirely in the reduction of cycle count, which reduces throughput time and capital equipment utilization per unit.

8. Conclusion

This paper has established the theoretical framework for applying Generated Pattern Current to hybrid capacitor production activation. The HyCap activation problem presents three concurrent physical processes that are not addressable by temporally uniform stimulation: ion diffusion into hierarchical pore structures, graphene contact network stabilization through micro-annealing, and synchronization of two electrodes operating at different characteristic timescales.

GPC addresses all three through a single parameterized composite current profile: diffusion relaxation intervals enable deep pore ion distribution; controlled pulse sequences drive systematic contact annealing; and frequency-domain component separation delivers stimulation at the natural timescale of each electrode type. Theoretical analysis predicts 60–80% reduction in activation cycle count, 10–20% reduction in ESR, 5–10% improvement in usable capacitance, and significantly narrowed cell-to-cell ESR variance in production batches.

HyCap activation is the fifth electrochemical domain in which the GPC paradigm has been analyzed—following lithium-ion battery formation, charging optimization, photovoltaic activation, and fuel cell conditioning. In each domain, the same core principle applies: nonlinearity of the electrochemical system means that the temporal structure of the applied current carries physical information that a time-averaged constant current cannot encode. Designing that temporal structure to match the target system's physical response characteristics is the defining capability of GPC.

The GigaPulse Lab platform provides a reference implementation enabling immediate experimental validation. Independent researchers with access to HyCap test environments are encouraged to conduct controlled comparisons using the proposed experimental protocol.

References

[1] I. Karakoc, "Dynamic Defined Pattern Charging (DDPC)," PCT/TR2025/051176; USPTO 19/298,223. Priority: July 23, 2025.

[2] B. E. Conway, Electrochemical Supercapacitors: Scientific Fundamentals and Technological Applications, Springer, 1999.

[3] P. Simon and Y. Gogotsi, "Materials for Electrochemical Capacitors," Nat. Mater., vol. 7, pp. 845–854, 2008.

[4] M. D. Stoller et al., "Graphene-Based Ultracapacitors," Nano Lett., vol. 8, pp. 3498–3502, 2008.

[5] Y. Zhu et al., "Carbon-Based Supercapacitors Produced by Activation of Graphene," Science, vol. 332, pp. 1537–1541, 2011.

[6] J. R. Miller and P. Simon, "Electrochemical Capacitors for Energy Management," Science, vol. 321, pp. 651–652, 2008.

[7] A. G. Pandolfo and A. F. Hollenkamp, "Carbon Properties and Their Role in Supercapacitors," J. Power Sources, vol. 157, pp. 11–27, 2006.

[8] E. Frackowiak, "Carbon Materials for Supercapacitor Application," Phys. Chem. Chem. Phys., vol. 9, pp. 1774–1785, 2007.

[9] P. Simon and Y. Gogotsi, "Charge Storage Mechanism in Nanoporous Carbons," J. Am. Chem. Soc., vol. 135, pp. 16818–16826, 2013.

[10] C. Zhong et al., "A Review of Electrolyte Materials for Electrochemical Supercapacitors," Chem. Soc. Rev., vol. 44, pp. 7484–7539, 2015.

[11] G. Wang et al., "A Review of Electrode Materials for Electrochemical Supercapacitors," Chem. Soc. Rev., vol. 41, pp. 797–828, 2012.

[12] V. Augustyn et al., "High-Rate Electrochemical Energy Storage Through Li+ Intercalation Pseudocapacitance," Nat. Mater., vol. 12, pp. 518–522, 2013.

[13] T. Brousse et al., "To Be or Not To Be Pseudocapacitive?," J. Electrochem. Soc., vol. 162, pp. A5185–A5189, 2015.

[14] D. Pech et al., "Ultrahigh-Power Micrometre-Sized Supercapacitors," Nat. Nanotechnol., vol. 5, pp. 651–654, 2010.

[15] M. F. El-Kady et al., "Laser Scribing of High-Performance Graphene Electrochemical Capacitors," Science, vol. 335, pp. 1326–1330, 2012.

[16] J. Chmiola et al., "Anomalous Increase in Carbon Capacitance at Pore Sizes Less Than 1 Nanometer," Science, vol. 313, pp. 1760–1763, 2006.

[17] C. Largeot et al., "Relation Between Ion Size and Pore Size for an EDLC," J. Am. Chem. Soc., vol. 130, pp. 2730–2731, 2008.

[18] R. Kotz and M. Carlen, "Principles and Applications of Electrochemical Capacitors," Electrochim. Acta, vol. 45, pp. 2483–2498, 2000.

[19] A. Burke, "Ultracapacitors: Why, How, and Where," J. Power Sources, vol. 91, pp. 37–50, 2000.

[20] M. Salanne et al., "Efficient Storage Mechanisms for Better Supercapacitors," Nat. Energy, vol. 1, p. 16070, 2016.

[21] H. Zhang and G. Cao, "Nanostructured Energy Materials," J. Mater. Chem. A, vol. 1, pp. 11221–11241, 2013.

[22] X. Yang et al., "Liquid-Mediated Dense Integration of Graphene Materials," Science, vol. 341, pp. 534–537, 2013.

[23] Z. Li et al., "Mesoporous Nitrogen-Rich Carbons," Energy Environ. Sci., vol. 6, pp. 871–878, 2013.

[24] E. Peled and S. Menkin, "Review—SEI: Past, Present and Future," J. Electrochem. Soc., vol. 164, pp. A1703–A1719, 2017.

[25] S. K. Heiskanen et al., "Generation and Evolution of the SEI," Joule, vol. 3, pp. 2322–2333, 2019.

Acknowledgments

The GPC-based hybrid capacitor activation protocol described in this paper is protected under PCT/TR2025/051176 and USPTO Application No. 19/298,223. The author is the named inventor. No external funding was received for the preparation of this manuscript.

Declaration of Competing Interest

Ibrahim Karakoc holds intellectual property and commercial rights related to the Generated Pattern Current (GPC) and Dynamic Defined Pattern Charging (DDPC) technology described in this paper through GigaPulse Energy, Izmir, Turkey.

Data Availability

Data will be made available on request.

Declaration on the Use of AI Writing Assistance

The authors used AI-assisted writing tools for language editing and manuscript preparation. The scientific content, theoretical analysis, and all intellectual contributions are entirely the work of the author. The author takes full responsibility for the integrity of the work.